Maja D. Obradović[1]*, Snežana Lj. Gojković[2]

[1]*University of Belgrade, Institute of Chemistry, Technology and Metallurgy, Belgrade, Serbia,* [2]*University of Belgrade, Faculty of Technology and Metallurgy, Belgrade, Serbia*

CO tolerant Pt/Ru$_{0.7}$Ti$_{0.3}$O$_2$ nanocatalyst for hydrogen oxidation reaction

ABSTRACT

The oxidation of pure H$_2$ and H$_2$/CO mixture (100 ppm CO) was investigated on Pt nanocatalyst supported on Ru$_{0.7}$Ti$_{0.3}$O$_2$ (Pt /Ru$_{0.7}$Ti$_{0.3}$O$_2$) by linear sweep voltammetry at a rotating disc electrode in 0.1 M HClO$_4$. The results were compared with those on the commercial Pt/C catalyst. It was demonstrated that Pt/Ru$_{0.7}$Ti$_{0.3}$O$_2$ electrode possesses good conductivity and stability of the supports in the electrochemical experiments. The onset potential of CO$_{ads}$ oxidation on Pt/Ru$_{0.7}$Ti$_{0.3}$O$_2$ is lower than Pt/C indicating that the Pt nanoparticles are in close contact with Ru atoms from support, which enable bifunctional mechanism and electronic effects to be operable. The influence of the poisoning of Pt/Ru$_{0.7}$Ti$_{0.3}$O$_2$ and Pt/C catalyst by CO$_{ads}$ on the HOR was examined at several surface coverages ranging from 0 to 0.6. The decrease in HOR current on CO$_{ads}$ poisoned surface in low over-potential region of 0.05-0.50 V is less pronounced on Pt/Ru$_{0.7}$Ti$_{0.3}$O$_2$ than on Pt/C. This is ascribed to a weakening of the Pt–CO interaction and consequently higher mobility of CO$_{ads}$ on Pt particles contacting Ru from the Ru$_{0.7}$Ti$_{0.3}$O$_2$ support.
***Keywords:** platinum, RuO$_2$, TiO$_2$, hydrogen oxidation, CO tolerance.*

1. INTRODUCTION

Proton exchange membrane fuel cells (PEMFC) have been demonstrated to be feasible energy converters that convert chemical energy of fuels, such as hydrogen, directly to electrical energy with high power density, high efficiency, and low to zero emissions. To date, carbon-based supporting materials are considered as the most practical supports for PEMFC catalysts. However, carbon oxidation in the presence of O$_2$ and/or at high electrode potential is inevitable, which causes performance degradation of PEMFCs [1]. This problem initiated numerous studies of alternative supporting materials with higher corrosion resistance under the PEMFC operating conditions.

Besides high corrosion resistivity, a catalyst support has to possess excellent electronic conductivity, uniform particle size distribution, high surface area, strong adhesive force to catalyst

particles, easy formation of uniform dispersion of catalyst particles on their surface etc. [2, 3]. In addition, for the non-carbon supporting materials the strong physicochemical and electronic interactions with catalytic metals are desirable in order to improve their catalytic activity and durability [3, 4]. The materials currently investigating as non-carbon support materials for fuel cell catalysts mostly include metal oxides, nitrides, carbides and conducting polymers [1, 3]. In the past several years TiO$_2$ has been successfully tested as a Pt catalyst support as a pure mesoporous oxide, doped by Nb [7-10] or as binary oxides such as Ti$_{0.7}$W$_{0.3}$O$_2$ [11], Ru$_x$Ti$_{1-x}$O$_2$ [12], hydrous and anhydrous TiO$_2$-RuO$_2$ [13] and Ti$_{0.7}$Ru$_{0.3}$O$_2$ [14,15]. The addition of foreign atoms into the TiO$_2$ crystal lattice increases the conductivity of otherwise low-conducting TiO$_2$ but can also promote the catalyst activity, i.e. transform a catalyst support to a co-catalyst.

TiO$_2$–mixed oxides with the ruthenium mole fraction over 0.27 were found to be electronically conducting, with conductivity increased with ruthenium mole fraction, and electrochemically stable [12,13]. Multifunctional binary metal oxide Ti$_{0.7}$Ru$_{0.3}$O$_2$ offers both excellent improvements in electrocatalytic activity and durability over

commercial carbon supported Pt and PtRu catalysts for direct methanol fuel cell. It was proven that presence of RuO$_2$ in catalyst support modify the electronic nature of the metal Pt particles, thus affecting their chemisorptive and catalytic properties. In additional, thanks to oxophilic properties of RuO$_2$, Ru sites provide oxygen-containing species at less positive potentials than Pt, hence facilitates oxidative removal of CO$_{ads}$, which acts as a catalyst poison [14].

The kinetics of hydrogen oxidation reaction (HOR) is of prime importance in PEMFC techno-logy in order to define the electrocatalyst optimum operation and effect of electrocatalyst deactivation (sintering, poisoning, reactant diffusion losses) on the fuel cell performance [16-28]. PEMFCs usually require platinum group metal (Pt, Ir, Rh, Pd) or its alloy as the anode electrocatalyst which has a high electrocatalytic activity for H$_2$ oxidation at a low temperature [29]. The role of CO in the poisoning of the H$_2$ dissociation reaction is of fundamental interest because hydrogen produced by reforming hydrocarbons usually contains small amount of CO, and CO has been shown to be a serious poison for HOR on Pt. Alloying of Pt with more oxofilic metals, like Ru, Sn, Mo, Re, W leads to CO oxidation at significantly lower overpotentials compared to pure Pt [18-20]. In addition, the influence of non-carbon supporting materials on electrochemical oxidation H$_2$/CO mixtures has been investigated on Pt nanoparticles supported on sub-stoichiometric titanium oxide [25], RuO$_2$–TiO$_2$ [14], tungsten carbide [26], etc. Superior CO tolerance of Pt in the presence of Ru was attributed to a bifunctional mechanism and electronic effect on CO oxidation, with the former one being predominant [28].

We recently reported that Pt/Ru$_{0.7}$Ti$_{0.3}$O$_2$ operate as a co-catalyst, enabling efficient methanol oxidation reaction (MOR) on the supported Pt nanoparticles [30]. Binary oxide Ru$_{0.7}$Ti$_{0.3}$O$_2$ was synthesized by an acid-catalyzed sol-gel method proposed for TiO$_2$ nanoparticles [31] and modified by addition of Ru [32]. Pt/Ru$_{0.7}$Ti$_{0.3}$O$_2$ catalysts with a nominal Pt loading of 20 mass% was prepared by modified borohy-dride reduction method [33]. It was shown [30] that oxide Ru$_{0.7}$Ti$_{0.3}$O$_2$ consisted of two phases with anatase and rutile structures with the predomi-nance of rutile phase. The Pt nanoparticles were around 3.7 nm in diameter and they were deposited on both Ru and Ti rich domains. Owing to close contact of RuO$_2$ in catalyst support and the Pt particles, bifunctional mechanism was enabled, which made the catalyst highly active for MOR. This result has led us to investigate HOR in absence and presence of CO$_{ads}$ at the same catalyst.

2. EXPERIMENTAL

The details of the synthesis of the Ru$_{0.7}$Ti$_{0.3}$O$_2$ and Pt/Ru$_{0.7}$Ti$_{0.3}$O$_2$ powders, as well as their physico-chemical characterization, are given elsewhere [30].

For the electrochemical characterization, the Pt/Ru$_{0.7}$Ti$_{0.3}$O$_2$ catalyst was applied on a glassy carbon (GC) substrate in the form of a thin–film [34]. The GC electrode (Tacussel rotating disk electrode, 5 mm in diameter) was polished with Al$_2$O$_3$ slurry and washed ultrasonically with water. The ink was made by mixing of 6.5 mg of Pt/Ru$_{0.7}$Ti$_{0.3}$O$_2$ powder with 1 cm^3 of high purity water (Millipore, 18 MΩ cm resistivity) and 50 µL of the Nafion® solution (5 wt. %, 1100 E.W., Aldrich). After 1 h of agitation in an ultrasonic bath, 10 µL of the suspension was placed onto the GC electrode and left to dry overnight. The Pt loading on the electrode was 65 µg cm^{-2}. A sample of commercial Pt nanoparticles supported on XC–72R carbon provided by E-TEK, Pt/C, with the Pt loading of 20 mass% and Pt particles of 2.5 nm [35] was used as the reference electrocatalyst. The metal loading on the electrode was 20 µg cm^{-2} for Pt/C.

Electrochemical characteristics of the Pt/Ru$_{0.7}$Ti$_{0.3}$O$_2$ and Pt/C thin film were investigated by cyclic voltammetry in 0.1 M HClO$_4$ saturated by N$_2$. After immersion into the electrolyte, the electro-de was subjected to potential cycling between 0.03 and 1.0 V at the scan rate of 100 mV s^{-1} over 5 min. Then the electrode potential was held at 0.1 V and CO was bubbled through the electrolyte. After for 30 min, which is necessary period for formation of a monolayer of CO$_{ads}$, CO was replaced by N$_2$ atmosphere for additional 30 min and the potential was scanned in positive direction to oxidize CO$_{ads}$ layer at the scan rate of 20 mV s^{-1}. In this way the electrochemically active surface area (EASA) of Pt was determined from the charge of the CO$_{ads}$ oxidation for each particular catalyst layer. In the next step the electrode was transferred into another cell containing the same supporting electrolyte saturated by H$_2$ (for the HOR investi-gation at the CO-free surface) or saturated by H$_2$/CO mixture with 100 ppm CO (for the HOR investigation the CO-contaminated surface).

The polarization curves for HOR at the CO-free surfaces of Pt/Ru$_{0.7}$Ti$_{0.3}$O$_2$ and Pt/C were recorded potentiodynamically in the potential range from 0.0 to 0.20 V, at the electrode rotating from 400 to 3600 rpm. The potential was scanned in a positive going direction at the scan rate of 2 mV s^{-1}.

For the investigation of the CO-contaminated surface, the electrode potential was kept at 0.05 V for various time intervals, ranging from 60 to 420 min, to form sub-monolayers of CO$_{ads}$. Then the HOR polarization curves were recorded in the potential range from 0.0 to 0.20 V at various rotation rates, in the same manner as described above. In order to determine the CO coverage, θ(CO), the electrode was transferred into the first cell filled with the N$_2$ saturated supporting electrolyte and subjected to a positive going scan at the rate of 20 mV s^{-1} up to 1.0 V.

In a separate set of the experiments the polarization curves for HOR at both catalysts were recorded in a wide potential range, up to 1.0 V. The potential scan was carried out after the formation of CO$_{ads}$ sub-monolayer over 420 min.

The three–compartment electrochemical glass cells were used with a Pt wire as the counter electrode and a saturated calomel electrode as the reference electrode. All the potentials reported in the paper are expressed on the scale of the reversible hydrogen electrode (RHE). The electro-chemical instrumentation included a PAR model 263A potentiostat and PAR PowerCV software for data acquisition and analysis. All the measure-ments were carried out at 23 °C.

3. RESULTS AND DISCUSSION

3.1. CO$_{ads}$ oxidation on Pt/Ru$_{0.7}$Ti$_{0.3}$O$_2$ and Pt surface area determination

Stripping voltammogram of CO$_{ads}$ and the first subsequent cyclic voltammogram of Pt/Ru$_{0.7}$Ti$_{0.3}$O$_2$ and Pt/C are shown in Figure 1a and b, respectively. Voltammogram of Pt/Ru$_{0.7}$Ti$_{0.3}$O$_2$ is well centered and without inclination, demon-strating good conductivity of the Ru$_{0.7}$Ti$_{0.3}$O$_2$ support. Well-defined peaks for hydrogen adsorp-tion/desorption and Pt-oxide formation and reduction are observed on the Pt/Ru$_{0.7}$Ti$_{0.3}$O$_2$ voltammogram, similarly to the Pt/C catalyst. However, the voltammogram of Pt/Ru$_{0.7}$Ti$_{0.3}$O$_2$ features the pseudocapacitive current in so-called double layer region (between 0.4 V and 0.51 V), which originates in Ru-oxide present in the oxide supports. It should be noted that in contrast to Pt/Ru$_{0.7}$Ti$_{0.3}$O$_2$ surface, the voltammogram of the Pt-Ru solid solution show no distinctive hydrogen adsorption/desorption peaks [30], indicating that no mixing between Pt and Ru occurred during preparation of Pt/Ru$_{0.7}$Ti$_{0.3}$O$_2$ catalysts.

Stripping voltammogram of CO$_{ads}$ at Pt/C presented in Fig. 1b shows that the CO$_{ads}$ oxidation commences 0.62 V. A symmetrical single oxidation current peak is observed with a maximum at 0.77 V, typical of pure Pt electrode. The onset potential of the CO$_{ads}$ oxidation on Pt/Ru$_{0.7}$Ti$_{0.3}$O$_2$ is about

0.40 V (Fig. 1a), a significantly more negative than in the case of Pt/C. In addition, the peak is broad and consist of two overlapping peaks (at 0.60 V and 0.67 V) and tails towards positive potentials, similarly as on PtRu/C [30]. Earlier onset of CO$_{ads}$ oxidation on Pt/Ru$_{0.7}$Ti$_{0.3}$O$_2$ comparing with Pt/C and separation of the CO$_{ads}$ oxidation peaks suggests that some CO molecules are adsorbed onto Pt nanoparticles that are in close contact with Ru (oxidation peak at lower potential), while the others are adsorbed onto Pt nanoparticles rather far from Ru (oxidation peak at higher potential) [30,36].
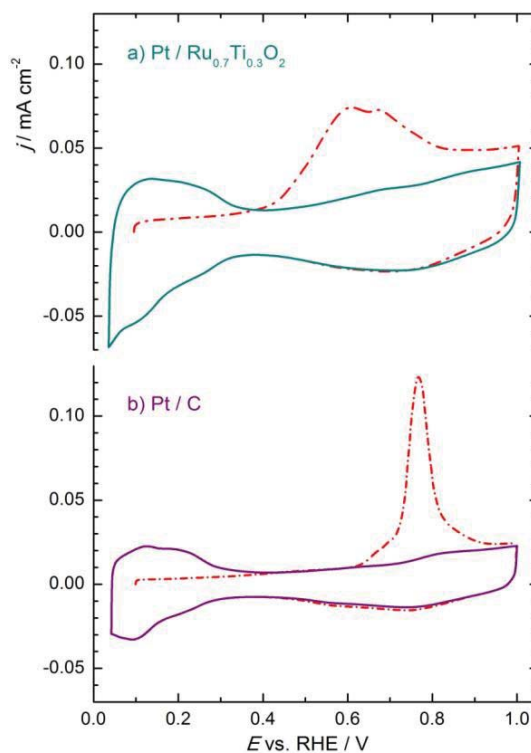

Figure 1. Stripping voltammograms of CO$_{ads}$ (dash-dotted lines) and the first subsequent cyclic voltammograms (solid lines) on a) Pt/Ru$_{0.7}$Ti$_{0.3}$O$_2$ and b) Pt/C. Data recorded in N$_2$ saturated 0.1 M HClO$_4$ at the scan rate of 20 mV s^{-1}.

Slika 1. Voltamogrami desorpcije CO (isprekidane linije) i prvi naredni ciklični voltamogrami za a) Pt/Ru$_{0.7}$Ti$_{0.3}$O$_2$ i b) Pt/C. Podaci snimljeni u 0,1 M HClO$_4$ zasićenom sa N$_2$ pri brzini promene potencijala od 20 mV s^{-1}.

Integration of the CO$_{ads}$ stripping voltammog-ram and the assumption that 420 µC cm^{-2} corres-ponds to a monolayer of CO$_{ads}$ enable estimation of EASA of Pt nanoparticles. At the beginning of each experiment the CO$_{ads}$ stripping voltammogram was recorded and EASA of Pt was determined. The cor-

rection for double layer capacitance, as recommended for metal-oxide supported Pt catalyst [37], was performed. The average EASA values from all the experiments carried out in the present study was normalized per mass of Pt on the electrode surface and the values of 46 m^2 g^{-1} and 87 m^2 g^{-1} were obtained for Pt/Ru$_{0.7}$Ti$_{0.3}$O$_2$ and Pt/C catalysts, respectively. Lower EASA for Pt/Ru$_{0.7}$Ti$_{0.3}$O$_2$ than for Pt/C is obtained because of difference in Pt particle size (3.7 nm and 2.5 nm) and because of rather pronounced agglomeration of Pt nanoparticles supported on Ru$_{0.7}$Ti$_{0.3}$O$_2$ [30].

3.2. HOR at Pt/Ru$_{0.7}$Ti$_{0.3}$O$_2$ without adsorbed CO

Polarization curves of hydrogen oxidation at Pt/Ru$_{0.7}$Ti$_{0.3}$O$_2$ as a function of rotating rate of RDE are presented in Fig. 2a. The HOR currents commence at 0.0 V, increase rapidly with potential and reach diffusion-limited current densities at approximately 0.06 V. Dependence of the diffusion-limited current densities on the rotation rate is given by the Levich equation [38]:

$$j_g = 0.62\, n\, F\, D^{2/3}\, v^{-1/6}\, c\, \omega^{1/2} = B\, \omega^{1/2} \qquad (1)$$

where j_g represents the diffusion-limited current density (with respect to geometric area od RDE), D is diffusion coefficient of hydrogen in solution, n is the number of electrons transferred in the HOR, v is kinematic viscosity of the electrolyte, c is the solubility of H$_2$ in solution and ω is the rotation rate of RDE (in rad s^{-1}). Diffusion-limited current densities of HOR at Pt/Ru$_{0.7}$Ti$_{0.3}$O$_2$ are presented as a Levich plot in Fig. 2 b). The linear dependence with zero intercept proves pure diffusion control of HOR.

Polarization data were analyzed in term of mass transport corrected Tafel diagrams. Assuming that the reaction is irreversible, mass transport corrected current densities are calculated as $j\, j_g/(j_g-j)$. In this calculation the EASA values were used. Fig. 2c shows Tafel diagrams for various rotation rates with the Tafel slope of ~30 mV dec^{-1}, which is typical for Pt surface [25, 27, 39]. For such value of the Tafel slope, dissociative adsorption of H$_2$ is generally accepted as the rate-determining step for HOR followed by very fast discharge step of adsorbed hydrogen, Tafel-Volmer pathway. Tafel-Volmer pathway is responsible for HOR activity on Pt at overpotential up to 0.05 V, while Heyrovsky-Volmer pathway is operative in the higher potential range [25, 26]. The HOR experiments were performed under the same conditions at Pt/C catalyst. It was found that the polarization curves and the Tafel plots (not shown) overlapped with those for Pt/Ru$_{0.7}$Ti$_{0.3}$O$_2$, indicating that the catalyst support does not influence the HOR kinetics.
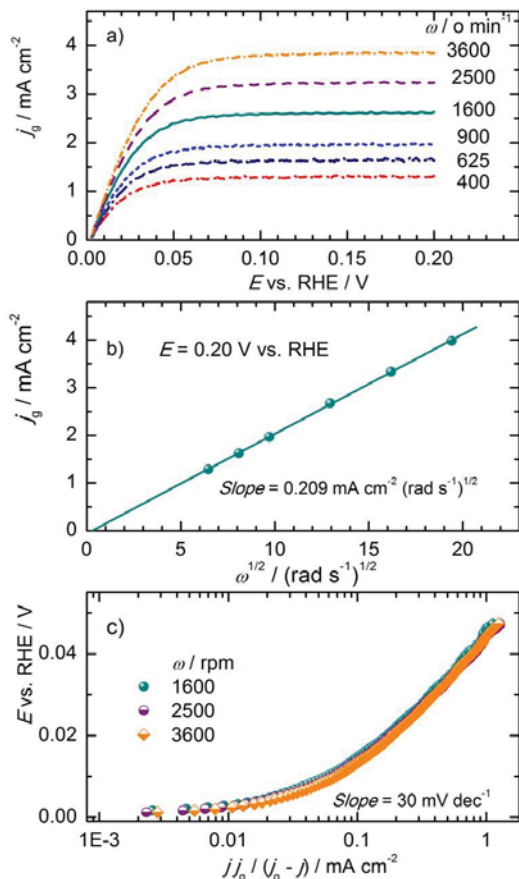

Figure 2. a) Polarization curves of HOR at Pt/Ru$_{0.7}$Ti$_{0.3}$O$_2$ in H$_2$ saturated solution 0.1 M HClO$_4$ as a function of rotation rate; data recorded at sweep rate of 2 mV s^{-1}; b) Levich plot, data taken at 0.2 V; c) Tafel plots at three different rotation rate.

Slika 2. a) Polarizacione krive oksidacije vodonika na Pt/Ru$_{0,7}$Ti$_{0,3}$O$_2$ u rastvoru 0,1 M HClO$_4$ zasićenom sa H$_2$, u zavisnosti od brzine rotiranja elektrode snimljene pri brzini promene potencijala 2 mV s^{-1}; b) odgovarajuća Levičeva zavisnost za gustine struje na 0,2 V; c) Tafelove zavisnosti na različitim brzinama rotiranja.

3.3. HOR at Pt/Ru$_{0.7}$Ti$_{0.3}$O$_2$ and Pt/C electrodes covered by CO$_{ads}$

Fig. 3a and b show typical anodic scans of cyclic voltammograms of Pt/Ru$_{0.7}$Ti$_{0.3}$O$_2$ and Pt/C electrodes with a pure surface and the surface partially covered by CO$_{ads}$. Owing to a decrease in the hydrogen desorption currents in the presence of CO$_{ads}$ on the Pt surface, the CO$_{ads}$ coverage can be determined by using the following equation, which is valid regardless of the type of CO adsorption, linear (on-top) or bridged (on two Pt atoms):

$$\theta(\mathrm{CO}) = \frac{Q(\mathrm{H^o}) - Q(\mathrm{H})}{Q(\mathrm{H^o})} \qquad (2)$$

where θ(CO) is CO$_{ads}$ coverage, while Q(H) and Q(H^o) are hydrogen desorption charges with and without CO$_{ads}$, respectively. It is worth noting that the shape of hydrogen desorption peaks on Pt/Ru$_{0.7}$Ti$_{0.3}$O$_2$ in presence of CO$_{ads}$ is also changed. The peaks are shifted toward more negative potentials and contribution of peak at more negative potential is higher than on bare surface as well as the same on Pt/C.
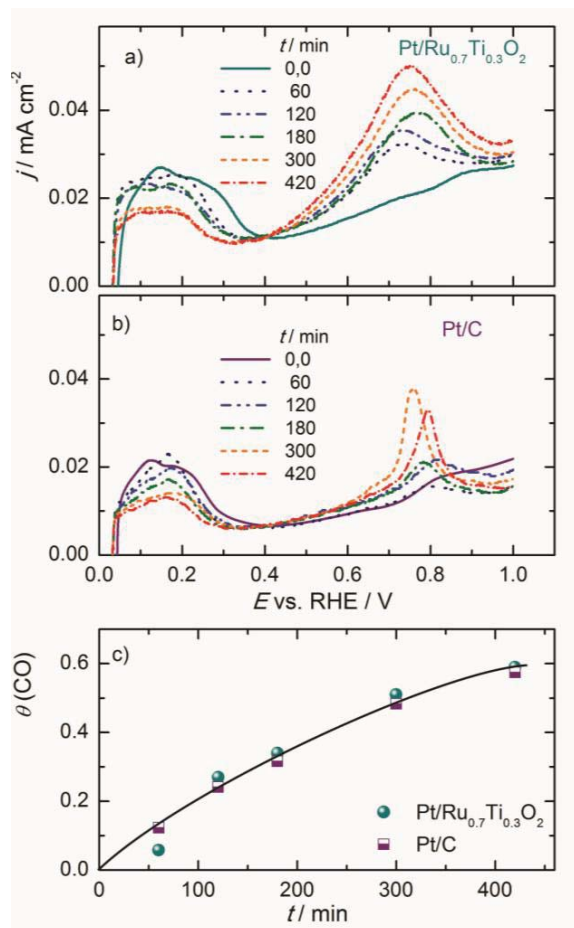

Figure 3. CO$_{ads}$ stripping voltammograms on a) Pt/Ru$_{0.7}$Ti$_{0.3}$O$_2$ and b) Pt/C as a function of time course for CO adsorption at the potential of 0.05 V in the H$_2$/CO saturated 0.10 M HClO$_4$; data recorded at the scan rate of 20 mV s^{-1}; c) CO$_{ads}$ surface coverage as function of time course for CO adsorption; data calculated from the voltammograms presented in diagrams a) and b)

Slika 3. Voltamogrami desorpcije CO$_{ads}$ na a) Pt/Ru$_{0.7}$Ti$_{0.3}$O$_2$ i b) Pt/C, u zavisnosti od vremena adsorpcije CO na potencijalu 0.05 V u rastvoru 0,1 M HClO$_4$ zasićenom smešom H$_2$/CO; brzina promene potencijala 20 mV s^{-1}; c) stepen pokrivenosti CO u zavisnosti od vremena adsorpcije CO računat na osnovu voltamograma prikazanim na slikama a) i b)

The dependence of CO$_{ads}$ coverage on the adsorption time for both catalysts is presented in Fig. 3c. As can be seen, CO$_{ads}$ coverage increases with the time course for CO adsorption with the values on Pt/Ru$_{0.7}$Ti$_{0.3}$O$_2$ and Pt/C being approximately the same for the same adsorption time. Assuming the simple Langmuir-type process for CO adsorption with desorption from the surface neglected, the adsorption rate is proportional to the number of free sites. In that case the linear relationship between log(1-θ(CO)) vs. time is expected with the slope proportional to the adsorption rate constant [17]. When data given in Fig. 3c are plotted in this way (not presented), well-defined linear relationships were obtained with approximately the same slopes for Pt on both supports.

The polarization curves for the HOR on pure Pt/Ru$_{0.7}$Ti$_{0.3}$O$_2$, as well as polarization curves for oxidation of H$_2$/CO mixture on Pt/ Ru$_{0.7}$Ti$_{0.3}$O$_2$ and Pt/C catalysts covered by CO$_{ads}$ with the approximately the same surface coverage are presented in Fig. 4. In forward scan the presence of CO$_{ads}$ on Pt surface leads to the significant decrease in the HOR current till potential of CO$_{ads}$ oxidation is reached. The decrease in the HOR current on Pt/Ru$_{0.7}$Ti$_{0.3}$O$_2$ is less pronounced than on Pt/C. At both electrodes at the potential around 0.4 V, where the oxidative removal of CO$_{ads}$ commences, the HOR currents start to increase and reach the diffusion-limited current density for pure HOR on uncontaminated Pt surface. In the backward scan, as the Pt surface is already freed of CO$_{ads}$, the currents are rather close to each other in the whole potential range. It should be noted that a small difference in the diffusion-limited current densities for the Pt/C and Pt/Ru$_{0.7}$Ti$_{0.3}$O$_2$ is a consequence of the method of the electrode preparation in which completely even distribution of the catalyst layer over the GC electrode is difficult to achieve.

The polarization curves of HOR at Pt/Ru$_{0.7}$Ti$_{0.3}$O$_2$ and Pt/C catalysts with bare and CO$_{ads}$ covered surface were also recorded in a narrow potential window that is relevant for the anode in H$_2$/O$_2$ PEMFC. The coverage of CO$_{ads}$ ranged from zero to ~0.6, which was attained by variation of the CO adsorption time. The results presented in Fig. 5 show that the HOR commences at 0.00 V at all the surfaces, but the potential at which the HOR reaches diffusion-limiting control is more negative for Pt/Ru$_{0.7}$Ti$_{0.3}$O$_2$ than for Pt/C surfaces of a similar CO$_{ads}$ coverage. The limiting current densities of HOR also depend on the CO$_{ads}$ surface coverage with lower values at the higher coverages. The decrease of HOR currents with the CO$_{ads}$ coverage is more pronounced on Pt/C than on Pt/Ru$_{0.7}$Ti$_{0.3}$O$_2$.
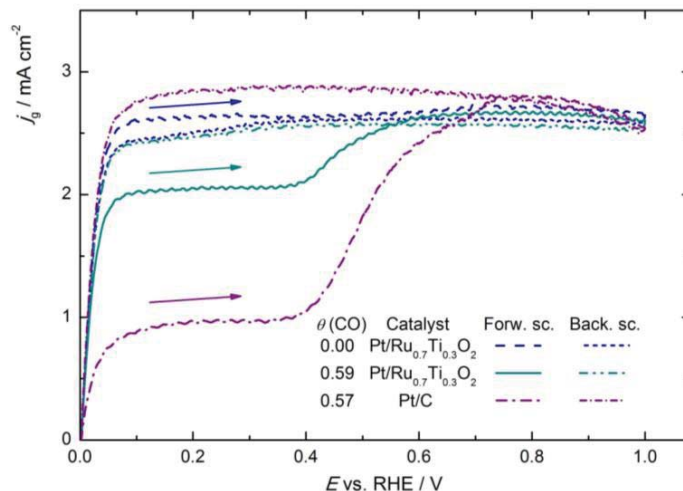
Figure 4. Polarization curves for the HOR on pure Pt/Ru$_{0.7}$Ti$_{0.3}$O$_2$ and on CO$_{ads}$ covered Pt/Ru$_{0.7}$Ti$_{0.3}$O$_2$ and Pt/C, with a similar surface coverage. The data were recorded in 0.1 M HClO$_4$ saturated by H$_2$ or H$_2$/CO mixture at the scan rate of 2 mV s^{-1} on the electrode rotated at 1600 rpm

Slika 4. Polarizacione krive za oksidaciju vodonika na Pt/Ru$_{0.7}$Ti$_{0.3}$O$_2$ i na površinama Pt/ Ru$_{0.7}$Ti$_{0.3}$O$_2$ i Pt/C pokrivenim sa CO$_{ads}$ pri sličnom stepenu pokrivenosti u rastvoru 0,1 M HClO$_4$ zasićenom smešom H$_2$/CO. Krive su snimljene pri brzini promene potencijala od 2 mV s^{-1} i pri brzini rotiranja elektrode od 1600 o min^{-1}
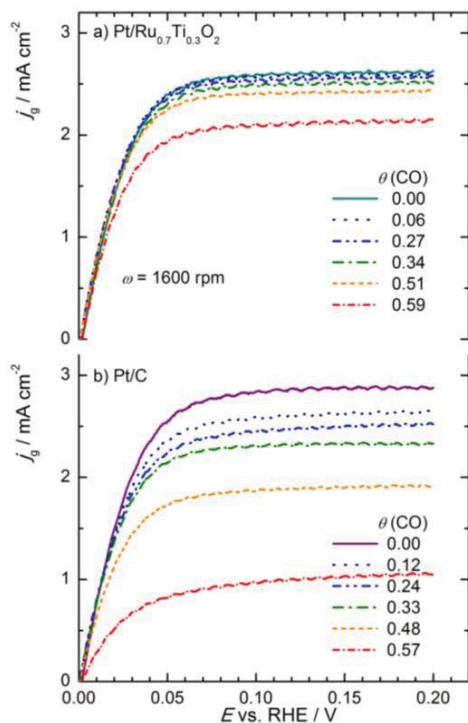

Figure 5. Polarization curves for the HOR on CO$_{ads}$ covered a) Pt/Ru$_{0.7}$Ti$_{0.3}$O$_2$ and b) Pt/C catalyst as function of CO$_{ads}$ surface coverage; data recorded in H$_2$/CO saturated 0.1 M HClO$_4$ at the potential scan rate of 2 mV s^{-1}

Slika 5. Polarizacione krive oksidacije vodonika na Pt/Ru$_{0.7}$Ti$_{0.3}$O$_2$ i Pt / C katalizatorima pri različitim stepenima pokrivenosti sa CO snimljene u rastvoru 0,1 M HClO$_4$ zasićenom smešom H$_2$/CO pri brzini promene potencijala od 2 mV s^{-1}

The decrease of HOR currents at high θ (CO) is probably due to the reduced number of neighboring two active (CO-free) sites required for H$_2$ dissociative adsorption in the rds. Higher current of HOR on CO$_{ads}$ covered Pt/Ru$_{0.7}$Ti$_{0.3}$O$_2$, doubling in value comparing to Pt/C at the same or similar surface coverage, indicates that the Pt active sites at the former catalyst are not so rigidly blocked by CO$_{ads}$ due to its easier mobility. Considering that CO$_{ads}$ on Pt/Ru$_{0.7}$Ti$_{0.3}$O$_2$ is not oxidized below 0.40 V (Fig. 1), it is reasonable to ascribe the increase in the mobility of CO$_{ads}$ to the weakening of the Pt–CO interaction owing to the electronic effect of Ru atoms from the Ru$_{0.7}$Ti$_{0.3}$O$_2$ support to the Pt atoms of the nanoparticles. As a result, the Ru$_{0.7}$Ti$_{0.3}$O$_2$ support acts as a co-catalyst improving Pt activity for HOR in the presence of CO, i.e. enhancing its CO-tolerance.

4. CONCLUSION

The activity of the synthesized catalyst Pt/Ru$_{0.7}$Ti$_{0.3}$O$_2$ for HOR and its CO tolerance were investigated and compared to the commercial Pt/C catalyst. It was shown that Pt/Ru$_{0.7}$Ti$_{0.3}$O$_2$ electrode possesses good conductivity and stability of the support in the electrochemical experiments. The onset potential of CO$_{ads}$ oxidation on Pt/Ru$_{0.7}$Ti$_{0.3}$O$_2$ is lower than on Pt/C, indicating that the Pt nano-particles are in close contact with Ru atoms from the support, which enable bifunctional mechanism to be operable. The kinetics of H$_2$ oxidation was found to be the same on Pt/Ru$_{0.7}$Ti$_{0.3}$O$_2$ and on Pt/C. The influence of the poisoning of Pt/Ru$_{0.7}$Ti$_{0.3}$O$_2$ and Pt/C catalyst by CO$_{ads}$ on the HOR rate was examined at CO$_{ads}$ surface

coverages up to ~0.6 in the wide potential range. The decrease in H$_2$ oxidation current on CO poisoned surface in low over-potential region of 0.05-0.50 V is more pronounced on Pt/C than on Pt/Ru$_{0.7}$Ti$_{0.3}$O$_2$. This was ascribed to a weakening of the Pt–CO interaction and the consequent increase in the mobility of CO$_{ads}$. Therefore, the Pt/Ru$_{0.7}$Ti$_{0.3}$O$_2$ catalyst is more CO-tolerant in HOR than the commercial Pt/C catalyst.

5. REFERENCES

[1] Y.-J. Wang, D.P. Wilkinson, J. Zhang (2011) Noncarbon support materials for polymer electrolyte membrane fuel cell electrocatalysts, Chem. Rev., 111, 7625–7651.

[2] Y. Shao, G. Yin, Y. Gao (2007) Understanding and approaches for the durability issues of Pt-based catalysts for PEM fuel cell, J. Power Sources, 171, 558–566.

[3] Y. Shao, J. Liu, Y. Wang, Y. Lin (2009) Novel catalyst support materials for PEM fuel cells: current status and future prospects, J. Mater. Chem., 19, 46–59.

[4] J. Zhou, X. Zhou, X. Sun, R. Li, M. Murphy, Z. Ding, X. Sun, T.-K. Sham (2007) Interaction between Pt nanoparticles and carbon nanotubes – An X-ray absorption near edge structures (XANES) study, Chem. Phys. Lett., 437, 229–232.

[5] S.-Y. Huang, P. Ganesan, S. Park, B.N. Popov (2009) Development of a titanium dioxide-supported platinum catalyst with ultrahigh stability for polymer electrolyte membrane fuel cell applications, J. Am. Chem. Soc., 131,13898–13899.

[6] S.-Y. Huang, P. Ganesan, B.N. Popov (2011) Titania supported platinum catalyst with high electrocatalytic activity and stability for polymer electrolyte membrane fuel cell, Appl. Catal. B-Environ., 102, 71–77.

[7] S.-Y. Huang, P. Ganesan, B.N. Popov (2010) Electrocatalytic activity and stability of niobium-doped titanium oxide supported platinum catalyst for polymer electrolyte membrane fuel cells, Appl. Catal. B-Environ., 96, 224–231.

[8] S.Lj. Gojković, B.M. Babić, V.R. Radmilović, N.V. Krstajić (2010) Nb-doped TiO2 as a support of Pt-Ru anode catalyst for PEMFCs, J. Electroanal. Chem., 639, 161–166.

[9] Q. Du, J. Wu, H. Yang. (2014) Pt@Nb-TiO$_2$ catalyst membranes fabricated by electrospinning and atomic layer deposition, ACS Catal., 4, 144−151.

[10] L. Chevallier, A. Bauer, S. Cavaliere, R. Hui, J. Roziere, D.J. Jones (2012) Mesoporous Nanostructured Nb-Doped Titanium Dioxide Microsphere Catalyst Supports for PEM Fuel Cell Electrodes, ACS Appl. Mater. Interfaces, 4, 1752−1759.

[11] D. Wang, C.V. Subban, H. Wang, E. Rus, F.J. DiSalvo, H.D. Abruña (2010) Highly Stable and CO-Tolerant Pt/Ti$_{0.7}$W$_{0.3}$O$_2$ Electrocatalyst for Proton-Exchange Membrane Fuel Cells, J. Am. Chem. Soc., 132, 10218–10220.

[12] O.E. Haas, T.S. Briskeby, O.E. Kongstein, M. Tsypkin, R. Tunold, B.T. Boressen (2008) Synthesis and characterisation of Ru$_x$Ti$_{x-1}$O$_2$ as a catalyst support for polymer electrolyte fuel cell, J. New Mat. Electrochem. Systems, 11, 9–14.

[13] C.-P. Lo, G. Wang, A. Kumar, V. Ramani (2013) TiO$_2$–RuO$_2$ electrocatalyst supports exhibit exceptional electrochemical stability, Appl. Catal. B-Environ., 140–141, 133–140.

[14] V.T.T. Ho, K.C. Pillai, H.-L. Chou, C.-J. Pan, J. Rick, W.-N. Su, B.-J. Hwang, J.-F. Lee, H.-S. Sheub, W.-T. Chuang (2011) Robust non-carbon Ti$_{0.7}$Ru$_{0.3}$O$_2$ support with co-catalytic functionality for Pt: enhances catalytic activity and durability for fuel cells, Energy Environ. Sci., 4, 4194–4200.

[15] V.T.T. Ho, N.G. Nguyen, C.-J. Pan, J.-H. Cheng, J. Rick, W.-N. Su, J.-F. Lee, H.-S. Sheu, B.-J. Hwang (2012) Advanced nanoelectrocatalyst for methanol oxidation and oxygen reduction reaction, fabricated as one-dimensional pt nanowires on nanostructured robust Ti$_{0.7}$Ru$_{0.3}$O$_2$ support, Nano Energy, 1, 687–695.

[16] W.Vogel, J. Lundquist, P. Ross, P. Stonehart (1975) Reaction pathways and poisons–II: The rate controlling step for electrochemical oxidation of hydrogen on Pt in acid and poisoning of the reaction by CO, Electrochim. Acta, 20,79–93.

[17] H. Igarashi, T. Fujino, M. Watanabe (1995) Hydrogen electro-oxidation on platinum catalysts in the presence of trace carbon monoxide, J.Electroanal. Chem., 391, 119–123.

[18] H.A. Gasteiger, N. Marković, P.N. Ross, E.J. Cairns (1994) CO electrooxidation on well-characterized Pt-Ru alloys, J. Phys. Chem., 98, 617-625.

[19] H.A. Gasteiger, N. Marković, P.N. Ross (1995) H$_2$ and CO electrooxidation on well-characterized Pt, Ru, and Pt-Ru. 1. rotating disk electrode studies of the pure gases including temperature effect, J. Phys. Chem., 99, 8290–8301.

[20] B. N. Grgur, N. M. Markovic and P. N. Ross (1998) Electrooxidation of H$_2$, CO and H$_2$/CO mixtures on a well-characterized Pt–Re bulk alloy electrode and comparison with other Pt binary alloys, Electroch. Acta, 43, 3631–3635.

[21] D.S. Strmcnik, P. Rebec, M. Gaberscek, D. Tripkovic, V. Stamenkovic, C. Lucas, N.M. Marković, (2007) Relationship between the surface coverage of spectator species and the rate of electrocatalytic reactions, J. Phys. Chem. C, 111, 18672–18678.

[22] G.A. Camara, E.A. Ticianelli, S. Mukerjee, S.J. Lee, J. McBreen (2002) The CO poisoning mechanism of the hydrogen oxidation reaction in proton exchange membrane fuel cells, J. Electrochem. Soc., 149, A748-A753.

[23] N.R. Elezović, Lj. Gajić-Krstajić, V. Radmilović, Lj. Vračar, N.V. Krstajić (2009) Effect of chemisorbed carbon monoxide on Pt/C electrode on the mechanism of the hydrogen oxidation reaction, Electrochim. Acta, 54, 1375–1382.

[24] N.R. Elezović, B.M. Babić, Lj.M. Vračar, V.R. Radmilović, N.V. Krstajić (2009) Preparation and characterization TiO$_x$–Pt/C catalyst for hydrogen oxidation reaction, Phys. Chem. Chem. Phys., 11, 5192–5197.

[25] B. Babić, J. Gulicovski, Lj. Gajić-Krstajić, N. Elezo- vić, V.R. Radmilović, N.V. Krstajić, Lj.M. Vračar (2009) Kinetic study of the hydrogen oxidation reaction on sub-stoichiometric titanium oxide- supported platinum electrocatalyst in acid solution, J. Power Sources, 193, 99–106.

[26] M.D. Obradović, S.Lj. Gojković, N.R. Elezović, P. Ercius, V.R. Radmilović, Lj.D. Vračar, N.V. Krstajić (2012) The kinetics of the hydrogen oxidation reaction on WC/Pt catalyst with low content of Pt nano-particles, J. Electroanal. Chem., 671, 24–32.

[27] N.R. Elezović, B.M. Babić, V. Radmilović, Lj.M. Gajić-Krstajić, N.V. Krstajić, Lj.M. Vračar (2011) A novel platinum-based nanocatalyst at a niobia- doped titania support for the hydrogen oxidation reaction, J. Serb. Chem. Soc., 76, 1139–1152.

[28] J.S. Spendelow, P.K. Babu, A. Wieckowski (2005) Electrocatalytic oxidation of carbon monoxide and methanol on platinum surfaces decorated with ruthenium,   Curr. Opin. Solid. St. M., 9, 37-48.

[29] J. Durst, C. Simon, F. Hasche, H.A Gasteiger (2015) Hydrogen oxidation and evolution reaction kinetics on carbon supported Pt, Ir, Rh, and Pd electrocatalysts in acidic media, J. Electrochem. Soc., 162, F190-F203.

[30] M.D. Obradović, U.Č. Lacnjevac, B.M. Babić, P. Ercius, V.R. Radmilović, N.V. Krstajić, S.Lj. Gojković (2015) Ru$_x$Ti$_{1-x}$O$_2$ as the support for Pt nanoparticles: Electrocatalysis of methanol oxidation, Appl. Cat. B: Environ.,170, 144–152.

[31] S. Boujday, F. Wunsch, P. Portes, J.F. Bocquet, C. Colbeau-Justin (2004) Photocatalytic and electronic properties of TiO$_2$ powders elaborated by sol–gel

route and supercritical drying, Sol. Energ. Mat. Sol. C., 83, 421–433.

[32] N.R. Elezović, B.M. Babić, V.R. Radmilović, Lj.M. Vračar, N.V. Krstajić (2013) Novel Pt catalyst on ruthenium doped TiO$_2$ support for oxygen reduction reaction, Appl. Catal. B-Environ., 140–141, 206– 212.

[33] K.W. Park, K.S. Seul (2007) Nb-TiO$_2$ supported Pt cathode catalyst for polymer electrolyte membrane fuel cells, Electrochem. Commun., 9, 2256–2260.

[34] T.J. Schmidt, H.A. Gasteiger, R.J. Behm (1999) Methanol electrooxidation on a colloidal PtRu-alloy fuel-cell catalyst, Electrochem. Communications, 1, 1–4.

[35] I. Esparbé, E. Brillas, F. Centellas, J.A. Garrido,R.M. Rodríguez, C. Arias, P.-L. Cabot (2009) Structure and electrocatalytic performance of carbon-supported platinum nanoparticles, J. Power Sources, 190, 201-209.

[36] Y.Y. Tong, H.S. Kim, P.K. Babu, P. Waszczuk, A. Wieckowski, E. Oldfield (2002) An NMR investi- gation of CO tolerance in a Pt/Ru fuel cell catalyst, J. Am. Chem. Soc., 124, 468–473.

[37] T. Binninger, E. Fabbri, R. Kotz, T.J. Schmidt (2014) Determination of the electrochemically active surface area of metal-oxide supported platinum catalyst, J. Electrochem. Soc., 161, H121-H128.

[38] A.J. Bard, L.R. Faukner (2001) Electrochemical Methods, John Wiley & Sons, New York (p. 339 and 341).

[39] B. E. Conway, B. V. Tilak (2002) Interfacial Processes Involving Electrocatalytic Evolution and Oxidation of H$_2$ and the Role of Chemisorbed H, Electrochim. Acta, 47, 3571–3594.

IZVOD

Pt/Ru$_{0,7}$Ti$_{0,3}$O$_2$ KAO NANOKATALIZATOR ZA OKSIDACIJU VODONIKA I NJEGOVA TOLERANCIJA NA CO

Oksidacija čistog H$_2$ i smeše H$_2$/CO (100 ppm CO) je ispitivana na nanokatalizatoru koji se sastojao od čestica Pt na nosaču Ru$_{0,7}$Ti$_{0,3}$O$_2$ (Pt/Ru$_{0,7}$Ti$_{0,3}$O$_2$). Korišćene su metoda linearne voltametrije u rastvoru 0,1 M HClO$_4$ i rotirajuća disk elektroda. Rezultati su upoređeni sa komercijalnim katalizatorom Pt/C. Za katalizator Pt/Ru$_{0,7}$Ti$_{0,3}$O$_2$ je utvrđena dobra provodnost i stabilnost nosača u elektrohemijskim eksperimentima. Pokazano je da oksidacija adorbovanog CO na Pt/Ru$_{0,7}$Ti$_{0,3}$O$_2$ počinje na negativnijim potencijalima nego na Pt/C. To ukazuje da su nanočestice Pt u bliskom kontaktu sa atomima Ru iz nosača, što omogućuje odigravanje bifunkcionalnog mehanizma i ispoljavanje elektronskog efekta. Uticaj trovanja katalizatora Pt/Ru$_{0,7}$Ti$_{0,3}$O$_2$ i Pt/C adsorbovanim CO na oksidaciju H$_2$ je ispitivan na nekoliko stepena pokrivenosti u opsegu od 0 do 0,6. Smanjenje struje oksidacije vodonika na površini delimično pokrivenoj adsorbovanim CO u oblasti malih prenapetosti 0,05-0,50 V je manje izraženo na Pt/Ru$_{0,7}$Ti$_{0,3}$O$_2$ u odnosu na Pt/C. Ovo se pripisuje slabljenju interakcija Pt–CO što dovodi do povećane pokretljivosti CO na česticama Pt koje su u kontaktu sa Ru iz nosača Ru$_{0,7}$Ti$_{0,3}$O$_2$.
***Ključne reči:** platina, RuO$_2$, TiO$_2$, oksidacija vodonika, tolerancija na CO.*